ROYAL SOCIETY OF CHEMISTRY

www.rsc.org/dalton

Synthesis of NaLuF$_4$-based nanocrystals and large enhancing upconversion luminescence of NaLuF$_4$: Gd, Yb, Er by coating an active shell for bioimaging

Juan Ouyang, Dongguang Yin*, Xianzhang Cao, Chengcheng Wang, Kailin Song, Bing Liu，

Lu Zhang, Yanlin Han, Minghong Wu*

College of Environmental and Chemical Engineering, Shanghai University, Shanghai 200444, China

*Corresponding author: ydg@shu.edu.cn

Abstract

A series of NaLuF$_4$-based hexagonal phase upconversion nanocrystals (UCNs) were synthesized by a facile solvothermal method and the properties of the UCNs were investigated. The results show that the as-prepared nanocrystals exhibit pure hexagonal lattice structures, uniform morphologies, high monodispersities and excellent upconversion luminescences. The upconversion luminescence (UCL) intensities of the UCNs can be enhanced by coating a shell of NaLuF$_4$. More interestingly, the UCL intensities of active-shell coated nanocrystals (NaLuF$_4$:Gd, Yb, Er @NaLuF$_4$:Yb, Ho and NaLuF$_4$:Gd, Yb, Er @NaLuF$_4$:Yb) are remarkable higher than that of inert-shell coated nanocrystals (NaLuF$_4$:Gd, Yb, Er@NaLuF$_4$), and NaLuF$_4$:Gd, Yb, Er @NaLuF$_4$:Yb, Ho is higher than NaLuF$_4$:Gd, Yb, Er @NaLuF$_4$:Yb. The mechanisms of upconversion luminescence enhancement were discussed in detail. The bioimaging application of the nanocrystals showed that bright upconversion luminescence was observed when UCNs-labeled HeLa cells were excited with 980nm light. This study presents a facile method for synthesis of NaLuF$_4$-based upconversion nanocrystals with intense luminescence that can be used as potential fluorescent probes for sensitive bioimaging, and the suggested mechanism could provide new insights into fabrication of upconversion materials with high upconversion fluorescence.

1. Introduction

In recent years, the upconversion nanocrystals (UCNs) have been attracted much attention and wildly used in optics, biology and medicine etc.[1-5] owing to their distinct optical and chemical properties such as large anti-Stokes shift, higher signal-to-noise ratio, deep penetration, non-toxic and high chemical stability.[6-9] However, the UCL efficiency and fluorescent intensity of the UCNs are usually low, leading their applications are still limited.[10-12] Improvement of the UCL efficiency is vital important for the applications of the UCNs, especially for high sensitive bioimaging and fluorescent immunoassay.

Among the lots of upconversion luminescence materials, $NaYF_4$ is usually regarded as the most efficient host matrix for lanthanide ions upconverting and,[13-15] $NaYF_4$:Yb, Er and $NaYF_4$:Yb, Tm are well-known as the most efficient upconversion nanocrystals.[16,17] However, there is still a big challenge to improve UCL efficiency of the $NaYF_4$-based nanocrystals for high sensitive bioimaging and assay.[18-20] Focus on development of alternative and better materials for $NaYF_4$-based UCNs is important, and has aroused great interest nowadays. In recent years, some reports proved that $NaLuF_4$ was a good host material for UCNs.[21] Li's group reported that lanthanide doped $NaLuF_4$ nanocrystals with size of 7.8 nm were more efficient than $NaYF_4$-based nanocrystals, and bright bioimaging in vivo was demonstrated.[22] Qin's group found that β-$NaLuF_4$:Yb, Tm UCNs showed intense ultraviolet and blue upconversion emission with longer fluorescence lifetime compared with $NaYF_4$-based one.[23] All of the above results demonstrate that $NaLuF_4$ is an excellent host for UCL.

Despite the promising UCL behavior and preliminary studies on $NaLuF_4$-based materials, there are only few reports on the study of lanthanide-doped $NaLuF_4$. Particularly, the study of $NaLuF_4$-based core-shell structural UCNs with lanthanide ions doped in the shell has not been reported. Therefore, it is highly desirable to further explore $NaLuF_4$-based UCNs with higher UCL, especially core-shell structural UCNs by optimizing their synthesis method and developing new nanocrystals structures.

In this work, a series of $NaLuF_4$-based UCNs were successfully synthesized and their UCL properties were investigated. These UCNs include core and core/shell nanocrystals, in which the shells involve insert-shell and active-shell. It is noticeable that this work is the first time to fabricate a novel core-shell structural nanocrystal $NaLuF_4$:Gd, Yb, Er@$NaLuF_4$:Yb, Ho with study of its bioimaging application, and compare the effects of insert-shell and active-shell on the UCL of the nanocrystals with discussion of their UCL mechanism. The as-prepared nanocrystal exhibiting superior upconversion

luminescence can be used as an effective luminescent nanoprobe for cancer cells bioimaging.

2. Experimental

2.1. Materials

Rare earth oxides Y_2O_3 (99.999%), Lu_2O_3 (99.999%), Yb_2O_3 (99.999%), Gd_2O_3 (99.999%), Ho_2O_3 (99.999%) and Er_2O_3 (99.999%) were purchased from Shanghai Yuelong New Materials Co. Ltd. Phosphate buffered saline (PBS),Oleic acid (>90%) and 1-octadecene were purchased from Sigma-Aldrich. NaOH, NH_4F, sodium citrate, diethylene glycol, hydrochloric acid, ethanol, methanol and cyclohexane were purchased from Enterprise group chemical reagent Co., Ltd. (Shanghai). $LnCl_3$ (Ln=Y, Lu, Gd, Yb, Er) were prepared by dissolving the corresponding metal oxide in hydrochloric acid at elevated temperature. All other chemical reagents with analytical grade were used directly without further purification.

2.2. Methods

2.2.1. Synthesis of the upconversion nanocrystals

Up to date, a lot of approaches for synthesizing upconversion nanocrystals have been developed, such as thermal decomposition, hydrothermal, solvothermal and ionic liquids methods.[24] Among these approaches, thermal decomposition using trifluoroacetate precursors has advantages of controllable of size and morphology. However, it exhibits drawbacks of rigorous reaction conditions, hazardous precursors and coordinating solvents. Hydrothermal can create highly crystalline phases at lower temperature. But it needs specialized reaction vessel such as autoclaves and the growing process of the nanocrystals is impossible to be observed. ionic liquid method has the merit of mild reaction condition and user-friendly regents, but exhibits drawbacks of poor shape-control and broad size distribution.[25,26] In compared with other methods, solvothermal method for synthesis of UCNs has advantages of mild reaction condition, toxic free, narrow size distribution and modulate-able shape.[27,28] The size of nanocrystals prepared by the solvothermal can be controlled through tuning the reaction temperature and time. In this study, solvothermal method was selected to synthesize UCNs. Furthermore, considering the Gd^{3+} ions can promote the transition of UCNs from cubic to hexagonal phase and increase the UCL intensity,[29-31] the Gd^{3+} ions were introduced as doping ions for the preparation of the UCNs. For

synthesizing NaLuF$_4$:Gd, Yb, Er nanocrystals, 1 mmol LnCl$_3$ (Ln= 54%Lu, 24%Gd, 20%Yb, 2%Er), 6 mL oleic acid (OA) and 15 mL 1-octadecene (ODE) were added to a 100 mL three-necked flask .The mixture was heated to 160 ºC to form a transparent solution, followed by cooling down to room temperature. Then 10 mL methanol solution containing 4 mmol NH$_4$F and 2.5 mmol NaOH was slowly added into the flask and stirred for 30 min. Subsequently, the solution was heated to 100 ºC and kept for 30 min to remove methanol and water, and then heated to 300 ºC under nitrogen atmosphere and kept for 1 h. After the solution was cooled down to room temperature, the desired nanocrystals were precipitated from the solution with ethanol, and collected after centrifuging and washing with ethanol for three times. The obtained products of NaLuF$_4$:Gd, Yb, Er were named as Lu1.

For synthesis of core-shell structural nanocrystals of NaLuF$_4$:Gd, Yb, Er@NaLuF$_4$ (named as Lu2), NaLuF$_4$:Gd, Yb, Er@NaLuF$_4$:Yb (named as Lu3) and NaLuF$_4$:Gd, Yb, Er@NaLuF$_4$:Yb, Ho (named as Lu4), 1 mmol LnCl$_3$ (Ln=100%Lu (for Lu2) or 80%Lu, 20%Yb (for Lu3), 79%Lu, 20%Yb, 1.0%Ho (for Lu4)), 6 mL oleic acid (OA) and 15 mL 1-octadecene (ODE) were added to a 100 mL three-necked flask. The mixture was heated to 160 ºC to form a transparent solution and then cooled down to 80 ºC. A solution of 1 mmol of prepared Lu1 (NaLuF$_4$:Gd, Yb, Er) in 4 mL of cyclohexane was added to the flask. After removing cyclohexane, 10 mL of methanol solution containing 2.5 mmol NaOH and 4 mmol NH$_4$F was slowly added into the flask and stirred for 30 min at room temperature . Subsequently，the solution was heated to 100 ºC and kept for 30 min to remove methanol and water, then heated to 300 ºC under nitrogen atmosphere and kept for 1 h. After the solution was cooled down to room temperature, the desired nanocrystals were precipitated from the solution with ethanol, and collected after centrifuging and washing with ethanol for three times. The obtained products were named as Lu3 and Lu4, respectively.

2.2.2. Synthesis of Hydrophilic sodium citrate-coated NaLuF$_4$:Gd, Yb, Er@NaLuF$_4$:Yb, Ho （Cit-Lu4）

The above prepared UCNs in oleic acid are hydrophobic which can only be dispersed in non-polar solvents. In order to perform its biomedical application, it should be transformed to hydrophilic. Here we used a ligand exchange method for rendering these UCNs dispersible in water [32]. A typical procedure is as follow: The mixed solution of diethylene glycol (DEG) (15.0 mL) and sodium citrate (2 mmol) was heated to 110 ºC for 30 min under nitrogen. Then, 10 mg Lu4 dispersed in chloroform and

toluene (v/v = 3:2) solution (5 mL) were injected into the above mixed solution and the system was heated to 160 ℃. After the chloroform and toluene had evaporated, the system was further heated to 220 ℃ for 3 h until the solution became clear. The resulting solution was cooled down to room temperature and treated with 0.1 M HCl aqueous solution, and the products were subsequently deposited. The precipitates were collected by centrifugation and washed three times with ethanol and deionized water, then the final citrate capped UCNs (abbreviated as Cit-Lu4) were dispersed in water.

2.2.3. Characterizations

The sizes and morphologies of nanocrystals were characterized by transmission electron microscope (TEM), which was performed on a JEOL JEM-2010F electron microscope operating at 200kV. Energy-dispersive X-ray analysis (EDX) of the samples was performed during high-resolution transmission electron microscopy (HRTEM) measurements to obtain the elements of samples. The crystal phase structures and compositions of the as-prepared samples were examined by powder X-ray diffraction (XRD) measurements which were performed on a Rigaku D/max-2500 X-ray diffractometer using Cu Kα radiation. The scan was performed in the 2θ range from 10° to 80° with a scanning rate of 8°/min. The upconversion luminescence emission spectra were recorded with an Edinburgh LFS-920 fluorescence spectrometer using an external 0-2W adjustable laser (980 nm, Beijing Hi-Tech Optoelectronic Co., China) as the excitation source instead of the Xenon source in the spectrophotometer. The images of upconversion luminescence were obtained digitally on a Nikon multiple CCD Camera. All the photoluminescence studies were carried out at room temperature. Upconversion luminescence lifetimes of the nanocrystals were measured with phosphorescence lifetime spectrometer (FSP920-C, Edinburgh) equipped with a tunable mid-band OPO pulse laser as excitation source (410-2400 nm, 10 Hz, pulse width ≤ 5 ns, Vibrant 355II, OPOTEK). Upconversion absolute quantum yields of the nanocrystals were measured according to the method reported by van Veggel and Zhang.[33,34] Fluorescence spectroscopy (Edinburgh LFS920) was modified by using Ocean Optics UV-VIS-NIR CCD (QE65000) as a detector for collecting the 980 nm light and the UC emissions upon 980nm NIR laser excitation at a power density of 25 W/cm^2. An integrating sphere was used to measure the efficiency data. The response of the detection systems in photon flux was determined using a calibrated VIS-NIR lamp (Ocean Optics LS-1-CAL). The quantum yield of UC emission of the nanoparticles was calculated with the following equation.

$$QY = \frac{\text{Photons emitted}}{\text{Photons absobed}} = \frac{E_{sample}}{A_{blank} - A_{sample}}$$

Where QY is the quantum yield, E_{sample} is the photons emitted per unit time of the sample in the UC emission range, A_{blank} and A_{sample} are the photons emitted per unit time by the excitation light in the absence and presence of the UCNPs samples, respectively.

2.2.4. Cytotoxicity assay

Cell viability was measured using a 3-(4,5-dimethylthiazol-2-yl)-2,5,-diphenyltetrazolium bromide (MTT) proliferation assay. Briefly, HeLa cells were seeded in a in a 96-well flat-bottomed microplate (6000 cells per well) and cultured in 100 μL growth medium at 37 ℃ and 5% CO_2 for 24 h. Cell culture medium in each well was then replaced by 100 μL cell growth medium, containing cit-Lu4 UCNs with concentrations ranging from 100 to 1000μg/mL. After incubation for 20 h, 20 μL MTT (5 mg/mL in PBS solution) was added to each well for further 4 h incubation at 37 ℃. The growth medium was removed gently by suction, and 200μL DMSO was then added to every well as solubilizing agent, sitting at room temperature overnight to dissolve the formazan crystals completely. The absorbance at the wavelength of 570 nm was measured by a Varioskan flash (Thermo Electron Corporation), and each data point was represented as mean ± standard deviation (SD) from triplicate wells.

2.2.5. Bioapplication of the nanocrystals for HeLa cells imaging

The confocal UCL imaging of HeLa Cells with the prepared UCNs was carried out as previous reported literature.[32] In typically, the HeLa cells were grown in MEM (Modified Eagle's Medium) supplemented with 10% PBS (Fetal Bovine Serum) at 37 ºC and 5% CO_2. Cells (5×10^8/L) were plated on 14 mm glass coverslips and allowed to adhere for 24 h. Before the experiments, HeLa cells were washed with PBS buffer (pH = 7) and then incubated with 300 μg/mL Cit-Lu4 at 37 ºC for 3 h. Cells imaging was performed with our laser scanning upconversion luminescence microscope.

3. Results and discussions

3.1. Structures, morphologies and compositions of the nanocrystals

The crystalline phases of the as-prepared samples were characterized by the powder XRD. As shown in Fig. 1, all of the products are all pure hexagonal phase crystals, indicating that $NaLuF_4$ host is apt to form

pure hexagonal phase, and the coated shell renders no influence on the crystal phase structure of the nanocrystals.

TEM and HRTEM images for the as-prepared nanocrystals are shown in Fig. 2. As shown in Fig. 2A, B, C and D, all of these as-prepared UCNs are uniform in morphology and size, and of high monodispersity. The average diameters of Lu1 is 27 ± 2 nm. After coating a $NaLuF_4$-based shell onto the core of $NaLuF_4$:Gd, Yb, Er (used as seeds), the diameter increases to 30 ± 2 nm, indicating the shell layer is epitaxially grown on the core nanocrystals. Every kind of UCNs are narrow size distribution. The morphologies of these nanocrystals shown in TEM images are in good agreement with the XRD results.

The HRTEM images of Lu1 (Fig. 2A，inset) and Lu4 (Fig. 2D, inset) reveal highly crystalline natures of the as-prepared nanocrystals. The determined values of interplanar distances between adjacent lattice fringes correspond to the crystal planes of the nanocrystals.[35,36] As shown in Figure 2D, the core and shell of Lu4 show the same crystalline characterizations due to their same matrixes.
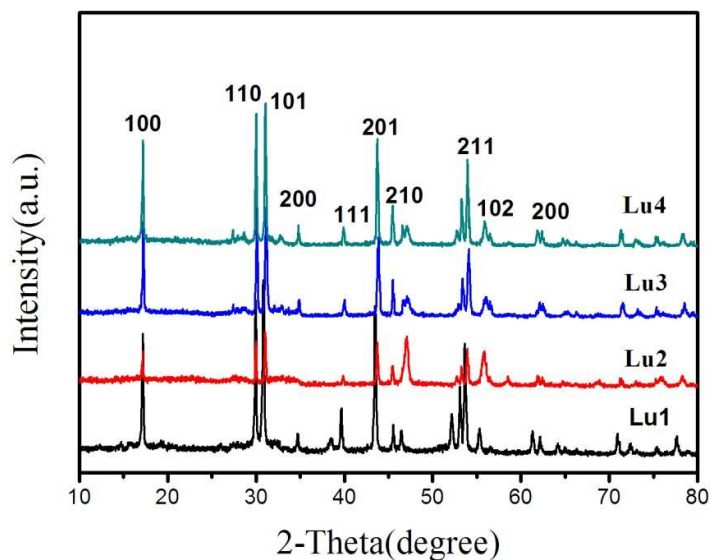
Fig. 1. XRD patterns of the as-prepared nanocrystals.
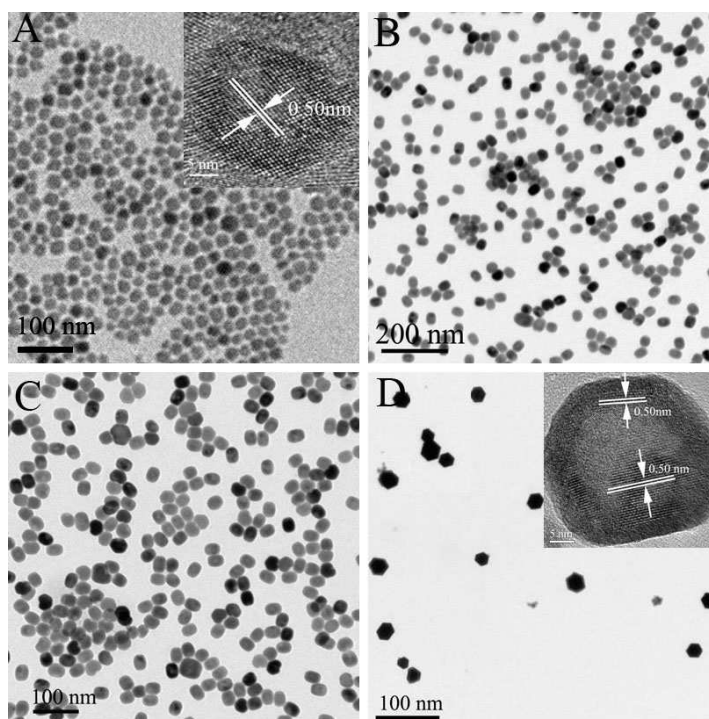
Fig.2. TEM and HRTEM images of the nanocrystals: Lu1 (A), Lu2 (B), Lu3 (C) and Lu4 (D)

The compositions of the core nanocrystal Lu1 (NaLuF$_4$:Gd, Yb, Er) and core/shell structural nanocrystal Lu4 (NaLuF$_4$:Gd, Yb, Er@NaLuF$_4$: Yb, Ho) are characterized by EDX analysis. As can be seen in Fig. 3A, all the elements of Lu1 including Lu, Gd, Yb and Er can be detected. Fig. 3B shows that upon growing a active shell NaLuF$_4$:Yb, Ho onto Lu1, new peaks at 5.98 KeV and 7.47 KeV emerge which correspond to the peaks of Ho, confirming that a Ho-doped shell has been coated onto the core and the core/shell structural nanocrystal Lu4 has been formed.

Fig. 3. EDX analysis of elemental compositions of (A) Lu1 (NaLuF$_4$:Gd, Yb, Er)
and (B) Lu4 (NaLuF$_4$:Gd,Yb, Er@NaLuF$_4$, Yb, Ho)

3.2. Upconversion luminescence properties of the nanocrystals

Fig. 4 shows the UCL spectra of the as-prepared nanocrystals. The UCL intensities of the prepared samples were measured at the same concentration of 1.0 mg/mL in cyclohexane. It can be seen that each of them shows typical characteristic UCL of Er^{3+}under CW excitation at 980 nm. The emission bands at 520 nm (green), 540 nm (green) and 654 nm (red) are corresponding to the $^2H_{11/2} \to$ $^4I_{15/2}$, $^4S_{3/2} \to$ $^4I_{15/2}$ and $^4F_{9/2} \to$ $^4I_{15/2}$ transitions of Er^{3+}, respectively.[32,36]

Fig. 4. Upconversion luminescence spectra of the as-prepared nanocrystals
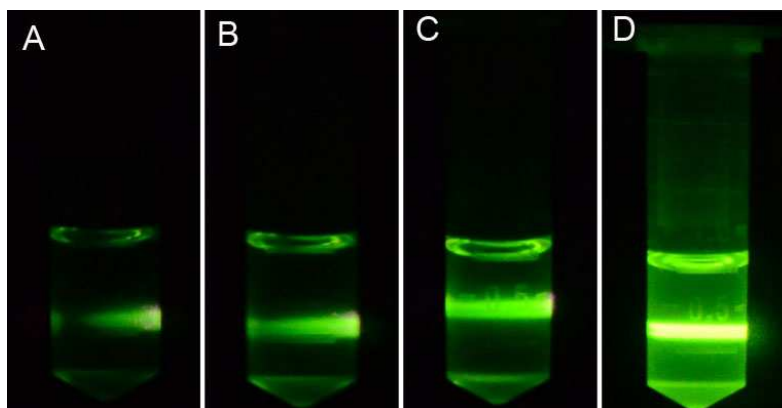
Fig. 5. Digital photographs of the nanocrystals in solution under the
excitation of a laser (980 nm). Lu1(A), Lu2(B), Lu3(C), Lu4(D)

As shown in Figure 5, strong upconversion fluorescence could still be easily observed by the naked eye when the solutions of these nanocrystals were excited with a commercial 980 NIR laser, demonstrating the prepared nanocrystals possess high upconversion fluorescence. Interestingly, the UCL intensities of the as-prepared nanocrystals are in the sequence (from weak to strong) of Lu1, Lu2, Lu3

and Lu4, which can be clearly seen from Figure 4 and 5.
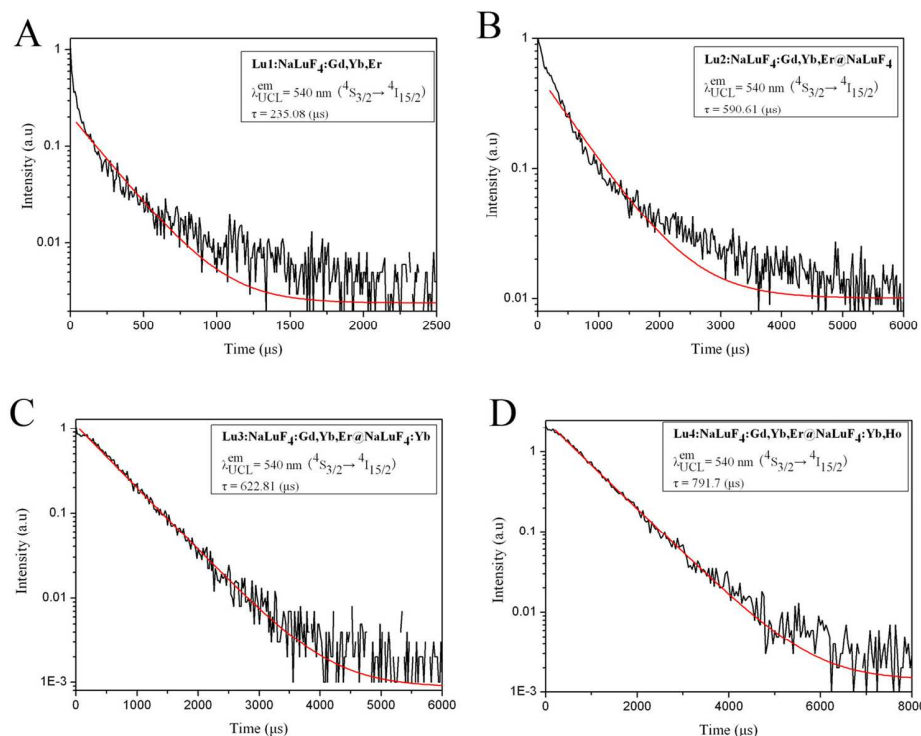
Fig. 6. UCL decays of the $^4S_{3/2} \rightarrow {}^4I_{15/2}$ transition of Er^{3+} in the Lu1 (A), Lu2(B), Lu3(C) and Lu4(D),respectively. All samples were all excited at 980 nm, and all the luminescence decay curves are fitted by using a single exponential function.

The UCL lifetimes of the nanocrystals were measured using 980nm excitation. As shown in Fig. 6, the measured UCL lifetimes of the $^4S_{3/2} \rightarrow {}^4I_{15/2}$ transition (corresponding to UCL at 540 nm) of Er^{3+} were 235.08, 590.61, 622.81 and 791.7 μs for Lu1, Lu2, Lu3 and Lu4, respectively. Usually, a long lifetime means a highly efficient UCL, and therefore, the enhanced UCL from Lu2, Lu3 and Lu4 is ascribed to the suppression of non-radiative processes in the crystal fields.[21,37]

The measured absolute UCL quantum yields of the nanocrystals are 0.07 ± 0.03 %, 0.28 ± 0.01 %, 3.2 ± 0.6 % and 5.4 ± 1.1 % for Lu1, Lu2, Lu3 and Lu4, respectively. Usually, the higher quantum yield is, the higher UCL efficiency will be.

The UCL intensities of Lu2, Lu3 and Lu4 are higher than that of Lu1, which can be attributed to the function of shell. During the epitaxial growth of the shell layer, surface defects of the nanocrystals can be gradually passivated by the homogeneous shell deposition process.[38,39] This protects the luminescent ions in the core (especially those near the surface) from non-radiative decay caused by surface defects as well as from vibrational deactivation from solvents or surface-bound ligands, resulting in the

11

enhancement of UCL.[40] Lu4 presents the highest UCL intensity among the 4 kinds of the as-prepared nanocrystals. Its UCL intensity is 2.5 times higher than that of Lu2. This result indicates that after coating an active shell (containing Yb^{3+} and Ho^{3+}) the UCL of the nanocrystals can be improved significantly. Furthermore, the active shell is more effective for enhancing UCL compared to the inert shell. In contrast to the inert-shell coated nanocrystal (Lu2), the difference is that the active-shell coated nanocrystal (Lu4) contain Yb^{3+} and Ho^{3+} (or Yb^{3+} for Lu3) which are doped in the shell. The mechanism of energy level and upconversion luminescence of Lu4 and the mechanism of emission enhancement are supposed as following descriptions. Fig. 7 shows the basic mechanism of upconversion fluorescence for the Lu4. Under the 980 nm excitation, the Yb^{3+} ion excited from the $^2F_{7/2}$ to the $^2F_{5/2}$ level and then drops back to the ground stated with transfer the energy to the adjacent Er^{3+}, which populates the $^4I_{11/2}$ level of Er^{3+} from the $^4I_{15/2}$ ground state. A second photon or energy transfer from an Yb^{3+} ion can then populate the $^4F_{7/2}$ level of the Er^{3+} ion.[41,42] The Er^{3+} ion can relax nonradiatively to the $^2H_{11/2}$ and $^4S_{3/2}$ levels, resulting in the observed green emission corresponding to the $^2H_{11/2} \rightarrow ^4I_{15/2}$ and $^4S_{3/2} \rightarrow ^4I_{15/2}$ transitions. Alternatively, the Er^{3+} ion can further relax and populate the $^4F_{9/2}$ level leading to red emission ($^4F_{9/2} \rightarrow ^4I_{15/2}$). The doped-$Yb^{3+}$ ion in shell can transfer the energy to the adjacent co-doped Ho^{3+}, which populates the $^5F_4$ and $^5S_2$ levels of Ho^{3+} from $^5I_6$ resulting in green emission corresponding to the $^5F_4 \rightarrow ^5I_8$ and $^5S_2 \rightarrow ^5I_8$ transitions. Alternatively, the energy transfer can populate the $^5F_5$ level of Ho^{3+} from $^5I_7$ resulting in red emission ($^5F_5 \rightarrow ^5I_8$).[43]

The sole role of the insert sell is to protect the luminescence core. However, the active shell has the functions which can not only protect the luminescence core, but also transfer energy to the core after absorbing NIR light from pump source.[44] As shown in Fig. 7, there are two kinds of energy transfers occurred between Yb^{3+} ion and Er^{3+} ion for the active shell coated nanocrystals, one is from the excited Yb^{3+} to the Er^{3+} in the core, another is from the excited Yb^{3+} in shell to the Er^{3+} in core. It means that the doped-Yb^{3+} in the active $NaLuF_4:Yb^{3+}$, Ho^{3+} shell can transfer its energy to the $NaLuF_4:Gd$, Yb, Er core,which cause the enhancement of the UCL. In addition, as shown in Fig. 7, there is another energy transfer occurred from excited Yb^{3+} to Ho^{3+} in shell for the active shell coated nanocrystals. This energy transfer causes a green emission and a weak red emission, corresponding to $^5F_4/^5S_2 \rightarrow ^5I_8$ and $^5F_5 \rightarrow ^5I_8$ transitions of Ho^{3+}.[45] Since the 543 nm of green emission wavelength of the Ho^{3+} almost overlaps the green emission wavelength of Er^{3+} (540 nm), resulting in raising the total UCL intensity. Furthermore, since the

Yb^{3+} ions are both doped in the core and shell, the increasing Yb^{3+} concentration at constant of Er^{3+} will also increase the UCL.[44,46] The concentration-dependent quenching can be avoided owing the Yb^{3+} in the core and those in the shell are spatially separated.[46]

For further confirming these suggested mechanisms, we prepared Lu3 in which Yb^{3+} are doped in shell but without Ho^{3+}. The result shows that the UCL intensity of Lu3 is higher that of Lu2 but lower than that of Lu4. Since there are Yb^{3+} ions doped in shell of Lu3, it causes the energy transfer from Yb^{3+} in shell to the Er^{3+} in core and enhancing the UCL (compared to Lu2). Whereas, there are no Ho^{3+} ions presented in the shell of Lu3, then no energy transfer occurred from Yb^{3+} to Ho^{3+} and no emission of Ho^{3+} in shell, leading the UCL of Lu3 lower than that of Lu4. These results reveal that coating an active shell over the core with doping suitable active Ln^{3+} ions in the shell is a facile and effective strategy to significantly increase the UCL of the nanocrystals.
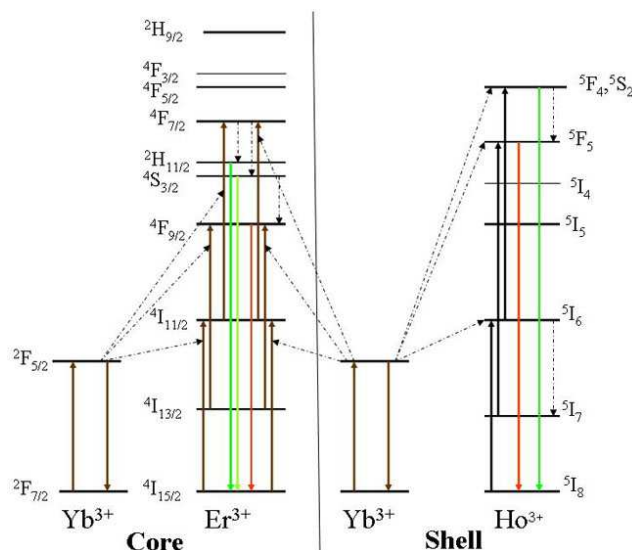
Fig. 7. Energy level and upconversion luminescence scheme
for the Lu4 ($NaLuF_4$:Gd,Yb, Er@$NaLuF_4$:Yb, Ho)

3.3. Cytotoxicity test

Toxicity is a critical factor determining the feasibility of the as-prepared nanoparticles in bioimaging applications. The viability of HeLa cells after exposure to cit-Lu4 UCNs with different concentrations was measured by a standard MTT assay. As shown in Fig. 8, the prepared UCNs of showed negligible cytoxicity toward HeLa cells, even at a high dosage of 1000 μg/mL for 24 h. The high viability of cells demonstrates the good biocompatibility and the potential of the UCNs for bioimaging applications.
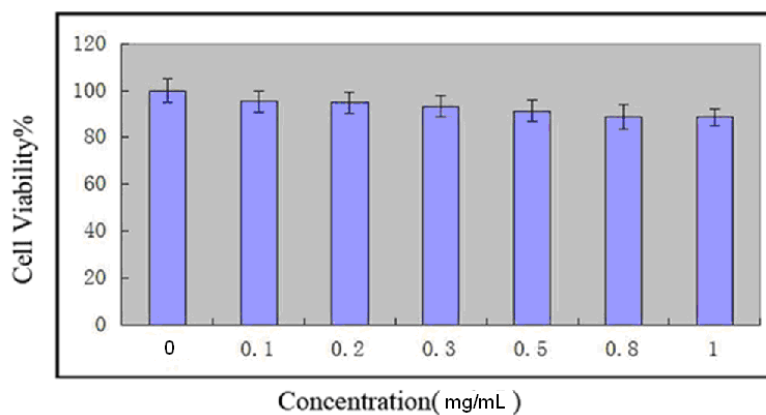
Fig.8. Viability of HeLa cells incubated with different concentrations of cit-Lu4 UNCs for 24h.

3.4. The application of UCL imaging of living cells in vitro

We explored the cellular uptake of the Cit-Lu4 by incubating HeLa cells with 300 μg/mL Cit-Lu4 in PBS buffer (pH = 7) at 37 ℃ for 3 h. Confocal microscopy images are shown in Fig. 9. As shown in Fig. 9B and C, strong UCL signals at 520-560 nm (green light) and 640-680 nm (red light) are detected. It can be seen from the overlay of confocal luminescence and bright-field images (Fig. 9D) that brightly luminescent aggregates are visible on the border of the cell membrane and inside of the cells, which indicate that the luminescence comes from the HeLa cells and the Cit-Lu4 has been internalized into the cells. These results imply that the UCNs Lu4 could be utilized as potential upconversion luminescence probe for bioimaging.
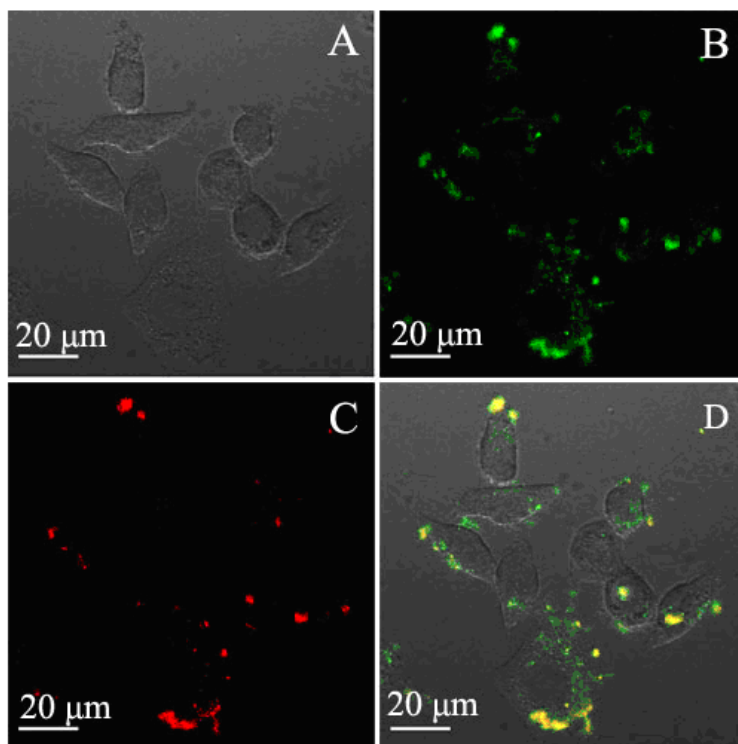
Fig. 9. Bright field image of HeLa cells(A), confocal images of HeLa cells after incubation with Cit-Lu4, collected at green (520-560 nm) (B) and red (640-680 nm) channels (C), and the overlay of bright-field image and panels B and C.

4. Conclusions

A series of $NaLuF_4$-based nanocrystals has been synthesized and characterized. The results show that in terms of the UCL intensities, the core-shell structured nanocrystals are higher than that of core, and the active-shell coated nanocrystals are higher than that of inert-shell coated nanocrystals. The synthesized novel active-shell coated nanocrystals $NaLuF_4$:Gd, Yb, Er@$NaLuF_4$:Yb, Ho show the highest UCL. These results reveal that the developed facile method, through coating an active-shell, can significantly improve the UCL of the nanocrystals. The successful application of the as-prepared UCNs in cells imaging demonstrates that the developed UCNs are potential luminescent nanoprobe which can be used in sensitive bioimaging.

References and notes

1 S. J. Zeng, J. J. Xiao, Q. B. Yang, and J. H. Hao, *J. Mater. Chem.* 2012, **22**, 9870.

2 J. Wang, H. W. Song, W. Xu, B. Dong, S. Xu, B. T. Chen, W. Yu, and S. Zhang, *Nanoscale* 2013, **5**, 3412.

3 D. Li, B. Dong, X. Bai, Y. Wang, and H. W. Song, *J. Phys. Chem. C* 2010, **114**, 8219.

4 S. Heer, K. Kompe, H. U. Gudel, and M. Haase, *Adv. Mater*. 2004, **16**, 2102.

5 J. F. Suyver, A. Aebischer, D. Biner, P. Gerner, J. Grimm, S. Heer, K W. Kramer, C. Reinhard, and H. U. Gudel, *Opt. Mater*. 2005, **27**, 1673.

6 L. M. Zhang, Z. X. Lu, Y. Y. Bai, T. Wang, Z. F. Wang, J. Chen, Y. Ding, F. Yang, Z. D. Xiao, S. H. Ju, J. J. Zhu, and N. Y. He, *J. Mater. Chem. B,* 2013, **9**, 128

7 M. Hintersteiner, A. Enz, P. Frey, A. L. Jaton, W. Kinzy, R. Kneuer, U. Neumann, M. Rudin, M. Staufenbiel and M. Stoeckli, *Nat. Biotechnol.* 2005, **27**, 577.

8 J. Zhou, Z. Liu, and F. Y. Li, *Chem. Soc. Rev.* 2012, **41**, 1323.

9 P. Tallury, K. Payton, S. Santra, and P. Sharma, *J. Biomed. Nanotechnol.* 2011*,* **7**, 724.

10 I. B. Neagoe, C. Braicu, C. Matea, C. Bele, G. Florin, K. Gabriel, C. Veronica, and A. Irimie. *J. Biomed. Nanotechnol.* 2012, **8**, 567.

11 L. Q. Xiong, M. Chen, Y. Sun, G. C. Guo, T. S. Yang, Y. Gao, X. Z. Zhang, and F. Y. Li, *Biomaterials* 2009, **12**, 30.

12 B. Sitharaman and L. J. Wilson, *J. Biomed. Nanotechnol.* 2007, **3**, 342.

13 A. Aebischer, M. Hostettler, J. Hauser, K. Kramer, T. Weber, H. U. Gudel, and H. B. Burgi, *Angew. Chem., Int. Ed.* 2006, **45**, 2802.

14 J. F. Suyver, A. Aebischer, S. Garcia-Revilla, P. Gerner, and H. U. Gudel, *Phys. Rev. B* 2005, **71**, 123.

15 Z. Li and Y. Zhang, *Nanotechnol.* 2008, **19**, 345606.

16 S. Tiwari, Y. M. Tan, and M. Amiji, *J. Biomed. Nanotechnol.* 2006, **2**, 217.

17 J. F. Suyver, J. Grimm, K. W. Krämer, and H. U. Güdel, *J. Lumin*. 2005, **114**, 53.

18 F. Wang, Y. Han, C. S. Lim, Y. Lu, J. Wang, J. Xu, H. Chen, C. Zhang, M. Hong and X. Liu, *Nature* 2010, **463**, 1061.

19 K. W. Krämer, D. Biner, H. U. Güdel, and S. R. Lüthi, *Chem. Mater.* 2004, **16**, 1244.

20 Q. Dou and Y. Zhang, *Langmuir* 2011, **27**, 13236.

21 T. S.Yang, Y. Sun, Q. Liu, W. Feng, P. Y. Yang, and F.Y. Li, *Biomaterials* 2012, **33**, 3733.

22 Q. Liu, Y. Sun, T. S. Yang, W. Feng, C. G. Li, and F. Y. Li, *J. Am. Chem. Soc.* 2011, **133**, 17122.

23 F. Shi, J. S. Wang, X. S. Zhai, D. Zhao, and W. P. Qin, *CrystEngComm.* 2011, **13**, 3782.

24 W. W. Wang and J. L. Yao, *J. Phys. Chem. C* 2009, **113**, 3070.

25 M. He, P Huang, C. L. Zhang, H. Y. Hu, C. C. Bao, G. Gao, F. Chen, C. Wang, J. B. Ma, R. He, and D. X. Cui, *Adv. Funct. Mater*. 2011, **21**, 4470.

26 M. He, P Huang, C. L. Zhang, J. Ma, R He, and D X Cui, *Chem. Eur. J.* 2012, **18,** 5954.

27 Y. J. Huang, H. P. You, J. Guang, Y. H. Zheng , Y. H. Song , M. Yang , K. Liu, and L. H. Zhang, *J. Phys. Chem. C* 2009, **113**, 16962.

28 L. Y. Wang and Y. D. Li, *Chem. Mater*. 2007, **4**, 727.

29 T. Jiang, Y. Liu, S. S. Liu, N. Liu, and W. P. Q *J. Colloid. Interf. Sci.* 2012, **377**, 81.

30 R. Kumar, N. Marcin, Y. Tymish, F. Christopher A, and P. Paras N, *Adv. Funct. Mater*. 2009, **19***,* 853.

31 J. P. Zhang, C. C. Mi, H.Y. Wu, H. Q. Huang, C. B. Mao, and S. K. Xu, *Anal. Biochem.* 2011*,* **421**, 673.

32 T. Y. Cao, T. S. Yang, Y. Gao, Y. Yang, H. Hu, and F. Y. Li, *Inrg. Chem. Commun.* 2010, **13**, 392.

33 J. C. Boyer and F. C. Van Veggel, *Nanoscale* 2010, **2**, 1417.

34 X. M. Li, D. K. Shen, J. P. Yang, C. Yao, F. Zhang, and D. Y. Zhao. *Chem. Mat.* 2013, **25**, 106.

35 H. X. Mai, Y. W. Zhang, L. D. Sun, and C. H. Yan, *J. Phys. Chem. C*, 2007, **111**, 13721.

36 C. X. Li, Z. W. Quan, P. P. Yang, S. S. Huang, H. Z. Lian, and J. Lin, *J. Phys. Chem. C* 2008, **112**, 13395.

37 Y. S. Liu, D.T. Tu, H. M. Zhu, R. F. Li, W. Q. Luo, and X.Y. Chen, *Adv. Mater.* 2010, **22**, 3266.

38 F. Zhang, R. C. X. Che, M. Li, C. Yao, J. P. Yang, D. K. Shen, P. Hu, W. Li, and D. Y. Zhao, *Nano Lett.* 2012, **12**, 2852.

39 H. Guo, Z. Li, and H. S. Qian, *Nanotechnol.* 2010, **21**, 125602.

40 H. Desirena, E. De la Rosa, P. Salas, C. Angeles, and R. Rodríguez, J. *Phys. D. Appl. Phys.* 2011, 44, 455308.

41 H. X. Mai, Y. W. Zhang, L. D. Sun, and C. H. Yan, *J. Phys. Chem. C* 2007, 111, 13721.

42 Y. S. Chen, W. He, H. H. Wang, X. L. Hao,Y. C. Jiao, J. X. Lu, and S. E. Yang. *J. Lumin.* 2012, **132**, 2404.

43 D. M. Yang, Y. L. Dai, P. A. Ma, X. J. Kang, M. M. Shang, Z. Y. Cheng, C. X. Li, and J. Lin. *J. Mater. Chem.* 2012, **22**, 20618.

44 F. Vetrone, R. Naccache, V. Mahalingam, A. Speghini, and J. A. Capobianco, Adv. *Mater.* 2009, **19**, 2924.

45 J. H. Chung, J. H. Ryu, S. Y. Lee, J. H. Lee, B. G. Choi, and K. B. Shim, *Mater. Res. Bull.* 2012, **47**, 1991.

46 Y. Mita, H. Yamamoto, K. Katayanagi and S. Shionoya, *J. Appl. Phys.* 1995, **78**, 1219.